Microstructure and Mechanical Properties of an α+β Type Ti-4V-0.60 Alloy

Materials Transactions, Vol. 58, No. 9 (2017) pp. 1250 to 1256

Microstructure and Mechanical Properties of an α+β Type Ti-4V-0.6O Alloy

Masahito Omiya*, Kyosuke Ueda and Takayuki Narushima

Department of Materials Processing, Tohoku University, Sendai 980–8579, Japan

This paper describes the design of a low-cost α+β type Ti-4V-0.6O alloy and the investigation of its microstructure and mechanical properties, with a focus on heat treatability. The β transus (T_β) of the alloy was found to be 1195 K, as determined from the relationship between the heat treatment temperature and the volume fraction of the equiaxed α phase (f_α). The formation of α' martensite exhibiting an acicular morphology was observed after heat treatments between 1073 and 1273 K. The O content in the equiaxed α and β phases increased with increasing heat treatment temperature while the V content increased with decreasing heat treatment temperature. The alloy demonstrated a higher tensile strength and lower total elongation when heat-treated between 1073 and 1173 K as compared to the as-forged material, because of the formation of α' martensite. The reduced total elongation was caused by the increase in the hardness difference between the equiaxed α and β (α' martensite) grains. The tensile strength and total elongation of the Ti-4V-0.6O alloy were comparable to those of the Ti-6Al-4V alloy, which marks the material as a low-cost α+β type Ti alloy candidate. [doi:10.2320/matertrans.L-M2017825]

(Received April 16, 2017; Accepted June 13, 2017; Published July 28, 2017)

Keywords: *α+β type titanium alloy, oxygen, heat treatment, distribution coefficient, mechanical properties*

1. Introduction

Ti and its alloys are used in aerospace components, chemical plants, and biomedical devices because of their high specific strength, excellent corrosion resistance, and biocompatibility[1]. The α+β type Ti alloys exhibit a wide range of mechanical properties, which are achieved by tailoring of the volume fraction and grain size of the equiaxed α phase through thermomechanical processing[2].

It is well known that the production cost of Ti and its alloys is high, and the utilization of ubiquitous elements has been suggested as an effective method of cost reduction for Ti alloys[3]. Oxygen (O), a ubiquitous element and the main impurity in Ti sponge, has a high chemical affinity with Ti, which makes purification of the metal difficult[4]. Therefore, utilizing O as an alloying element lowers the production cost of Ti alloys since low-grade Ti sponge and Ti scrap can be employed as raw materials.

The α phase stabilizability of O is thought to be 10 times larger than that of Al[5]. It is reported that the presence of O in Ti increases the hardness and tensile strength of the material, but decreases the ductility and fracture toughness[6–8]. Studies have previously been conducted on α+β type Ti alloys with a high O content. The commercial Super-TIX 800 alloy (Ti-1 mass% Fe-(0.3–0.35) mass% O-(0.01–0.05) mass% N)[9,10] is an α+β type Ti alloy which uses O as an α stabilizer. In this alloy, Fe is used as a β stabilizer, and is also one of the main impurity elements in Ti sponge. However, it is known that long-term use of this alloy at moderate temperatures leads to a reduction in the tensile strength and elongation, because of precipitation of the TiFe phase[9,10]. In comparison, V is a β-isomorphous type element and does not form any intermetallic compounds with Ti. Therefore, utilizing V as a β stabilizer is advantageous as it allows the use and heat-treatment of Ti-V-O alloys at moderate temperatures.

Our previous work investigated the microstructure and mechanical properties of α+β type Ti-(0–10) mass% V-(0.5–1) mass% O alloys using O as an alloying element[11]. The experiments revealed that the athermal ω was formed during quenching from the α+β region (923–1123 K) in the alloys with 6–10 mass% V, due to V enrichment in the β phase during heat treatment. Conversely, the Ti-4 mass% V-(0.5–0.75) mass% O alloys exhibited an excellent strength-ductility balance without the formation of the athermal ω. However, the effects of the heat treatment conditions on the mechanical properties of the Ti-V-O alloys have not been reported. Therefore, in this study, we designed a low-cost α+β type Ti alloy of composition Ti-4 mass% V-0.6 mass% O based on our previous findings (described above). The Al-equivalent in this alloy was set to equal that of the most commonly used Ti alloy, Ti-6 mass% Al-4 mass% V. The 0.6 mass% O content makes it possible to use raw materials with a high O content, such as low-grade Ti sponge and scrap. The objective of this study was to clarify the effects of heat treatment on the microstructure and mechanical properties of this α+β type Ti alloy. Hereafter, the chemical composition is denoted in mass%, and "mass%" notation is omitted.

2. Experimental Procedure

Commercially pure (CP) Ti (JIS Grade 2, UEX Ltd., Tokyo, Japan, O: 1038 mass ppm) and TiO_2 powder (99.5%, ϕ1 μm, Kanto Chemical Co. Inc., Tokyo, Japan) were melted using a non-consumable electrode Ar arc melting furnace to fabricate a master Ti-O binary alloy containing 1.6 mass% O. Following this, the master alloy, CP Ti, and V flakes (Kojundo Chemical Laboratory Co. Ltd., Sakado, Japan, O: 123 mass ppm) were arc-melted to fabricate a Ti-4V-0.6O alloy ingot. The O content in the alloy was measured by the inert gas fusion-infrared (IR) absorption method (ONH836, LECO, MI). The V, Fe, and Al contents were measured using inductively coupled plasma-mass spectrometry (ICP-MS, Agilent8800, Agilent technologies, CA), and the chemical composition of the alloy is shown in Table 1. After melting, the ingot was subjected to forging in the β region at 1373 K to a ϕ12 mm bar followed by air cooling to room

*Corresponding author, E-mail: masahito.omiya.t7@dc.tohoku.ac.jp

temperature, and then to forging in the α+β region at 1073 K to a ϕ8 mm bar, and again followed by air cooling to room temperature. During forging, the alloy was reheated to the forging temperature several times. Hereafter, the forged specimen is referred to as the "as-forged alloy." The as-forged alloy was cut into sections ($\phi 8 \times 40$ mm) and the residual oxide scale was removed by machining. The heat treatments were conducted in an Ar flow atmosphere at 873–1273 K for 3.6 ks, followed by ice-water quenching. Hereafter, the heat-treated specimen is referred to as the "heat-treated alloy."

The constituent phases of the heat-treated alloy were identified by X-ray diffraction (XRD, D8 ADVANCE, Bruker AXS K.K., Karlsruhe, Germany). The microstructure was observed by scanning electron microscope (SEM, VE-7800, Keyence Co., Osaka, Japan) after mirror polishing and etching in a 2 vol% HF + 13 vol% HNO_3 + 85 vol% H_2O solution. The volume fraction of the equiaxed α phase (f_α) was calculated from five SEM images (×2000) using image analysis software (ImageJ, NIH). The value of f_α was calculated as an area fraction of the equiaxed α phase observed in the SEM images, as defined by eq. (1):

$$f_\alpha = \frac{S_\alpha}{S_{\text{Total}}} \tag{1}$$

where S_α is the equiaxed α phase area found in the SEM image and S_{Total} is the total image area.

Further microstructure observation was conducted by transmission electron microscope (TEM, JEM-ARM200F, JEOL Ltd., Tokyo, Japan). The O and V contents of the equiaxed α and β phases were determined using a field emission electron probe microanalyzer (FE-EPMA, JXA-8530F, JEOL Ltd., Tokyo, Japan) with the CP Ti and Ti-(6, 10)V-(0.5, 1)O alloys as reference materials. Measurements were conducted at 10 positions for each phase and an average value and standard deviation were calculated.

The Vickers hardness of the as-forged and heat-treated alloys was obtained using a Vickers micro-hardness tester (HM-102, Mitsutoyo Co., Kanagawa, Japan) under a 50 gf load. As the grain size of each phase was approximately 2 to 3 μm, the hardness of each grain was measured by a nano-indentation hardness tester (ENT-1100a, ELIONIX Inc., Tokyo, Japan) with a 500 mgf load. After indentation testing, we observed the indentation trace using SEM. We did not employ the data in the case where the indentation trace was on both the α and β grains, so that the accuracy in our measurements could be improved. Uniaxial tensile tests were conducted at room temperature using a universal material testing instrument (RTF-1325, A&D Co. Ltd., Tokyo, Japan). The tensile specimens were machined to a gage diameter and length of 3 mm and 10 mm, respectively. The strain rate was set to 5.0×10^{-4} s^{-1}, and the tensile strength, 0.2% proof stress, and total elongation were measured. Tensile tests were conducted on three specimens for each heat treatment condition and average values and standard deviations were calculated.

Table 1 Chemical composition of the alloy used in this study (mass%).

Ti	V	O	Fe	Al
Bal.	3.435	0.638	0.034	0.004

3. Results

3.1 Microstructure of as-forged and heat-treated alloys

Figure 1 shows SEM images of the as-forged and heat-treated alloys after etching. The black regions visible in the alloys heat-treated from 873 to 1173 K are the equiaxed α phase. Both the as-forged alloy and the alloy heat-treated from 873 to 1173 K exhibit an equiaxed microstructure. The white regions of the microstructure found in the alloy heat-treated from 873 to 1023 K is the β phase, while a transformed microstructure exhibiting an acicular morphology was observed between 1073 and 1273 K. Using these SEM images, the associated f_α values were calculated and are plotted in Fig. 2 as a function of the heat treatment temperature (an approach curve). Equiaxed α phase was not observed in the alloy heat-treated at 1223 and 1273 K; therefore, the values of f_α for these specimens were plotted as

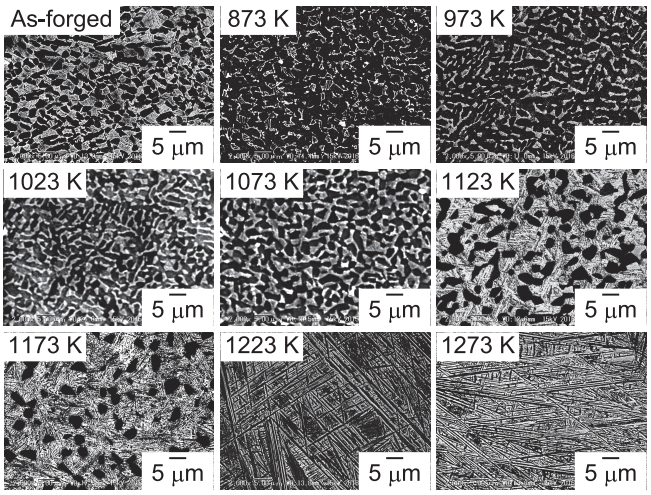

Fig. 1 Microstructure of the as-forged and heat-treated alloys.

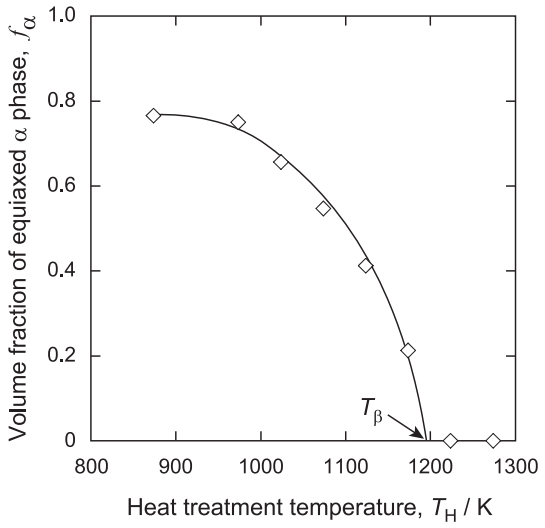

Fig. 2 Volume fraction of equiaxed α phase (f_α) occurring in the alloy heat-treated at various temperatures.

zero in this figure. The value of f_α decreased with increasing heat treatment temperature. The β transus (T_β) of the alloy was estimated to be 1195 K, by extrapolation of the approach curve to $f_\alpha = 0$.

The XRD patterns obtained from the heat-treated alloy are shown in Fig. 3. Hexagonal close-packed (hcp) peaks were detected in all specimens and the β phase peak was detected in specimens heat-treated between 873 and 1023 K. Peak separation of the hcp phase was observed in the alloy after heat treatment at 1073 and 1123 K (as shown by arrows in Fig. 3), but not after heat treatment at other temperatures. The heat treatment temperatures of 1223 and 1273 K were above the T_β of this alloy. The acicular structure (Fig. 1) and hcp peaks (Fig. 3) observed in the heat-treated alloy suggest that the β phase observed at 1223 and 1273 K transformed to α' martensite (hcp) during quenching. Similarly, the formation of α' martensite is indicated in the alloys heat-treated from 1073 and 1273 K.

3.2 Composition of equiaxed α and β phases after heat treatment

The O and V contents of the equiaxed α and β phases of the alloys heat-treated from 1023 to 1173 K are shown in Fig. 4, plotted as a function of heat treatment temperature. The dashed lines in the figures represent the O and V contents of the entire alloy, measured by the inert gas fusion-IR absorption and ICP-MS methods, respectively. The O content in equiaxed α and β phases increased with increasing heat treatment temperature, achieving a maximum of 0.87 mass% in the equiaxed α phase at 1173 K. Conversely, the V content in the equiaxed α and β phases increased with decreasing heat treatment temperature, reaching 8.92 mass% in the β phase at 1023 K. When the heat treatment temperature decreases, the size of the β grains decreases. In addition, the larger the difference in element content between the α and β grains, the greater will be the error in the EPMA analysis. In this context, the most concerned analysis in accuracy will be the measurement of the V content in the β grains of the alloy heat-treated at 1023 K. Under this condition the standard deviation in analysis was 0.79 mass% (V content: 8.92 ± 0.79 mass%), which suggests a relatively good accu-

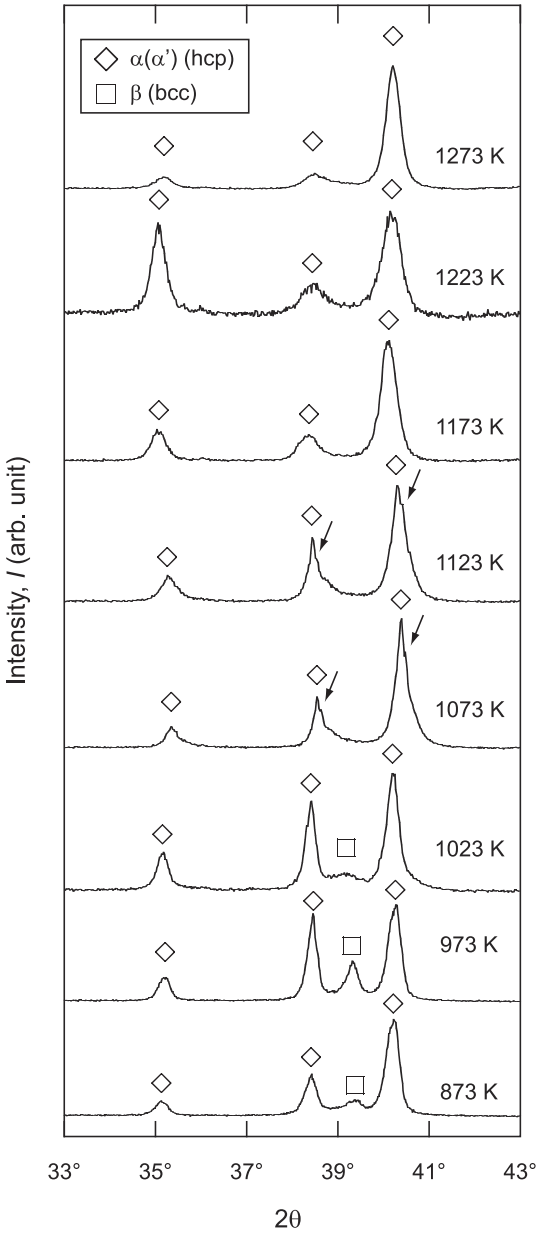

Fig. 3 X-ray diffraction (XRD) patterns of the alloy heat-treated at various temperatures.

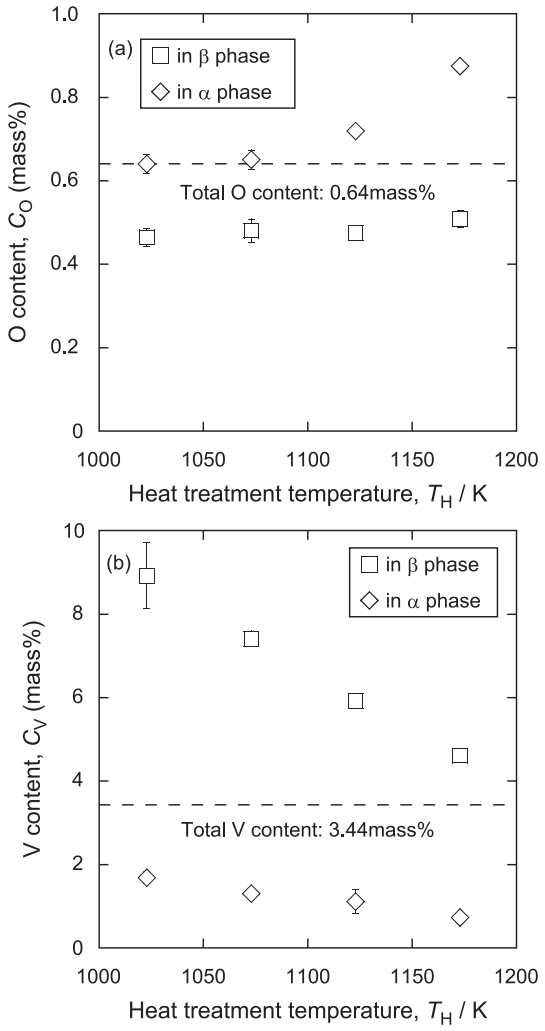

Fig. 4 Change in (a) O and (b) V contents in the equiaxed α and β phases with heat treatment temperature.

racy in our EPMA analysis. This is because, as described in the Experimental section, we determined the V and O values in EPMA analysis by using a calibration curve with reference CP Ti and Ti alloys having a uniform composition.

3.3 Mechanical properties of the as-forged and heat-treated alloys

The stress-strain curves of the as-forged and heat-treated alloys are shown in Fig. 5. While the as-forged alloy and the alloy heat-treated from 973 to 1173 K exhibited plastic deformation region, the specimens heat-treated at 1223 and 1273 K did not. The tensile strength, 0.2% proof stress, and total elongation values of the as-forged and heat-treated alloys are summarized in Fig. 6. The tensile strength of the alloy heat-treated from 1073 to 1173 K was higher than that of the as-forged alloy, but the tensile strength subsequently decreased when the heat treatment temperature increased to 1223 and 1273 K. A similar tendency was observed in the 0.2% proof stress results. Based on Figs. 5 and 6, the difference in the alloys' tensile strength and 0.2% proof stress is evidently small, and the work hardening is unremarkable in the α+β region.

The Vickers hardness values of the as-forged and heat-treated alloys are shown in Fig. 7. The Vickers hardness increased with increasing heat treatment temperature, from 337 Hv at 873 K to 369 Hv at 1173 K.

The relationship between the heat treatment temperature and indentation hardness of the equiaxed α and β (α') grains (as measured using a nano-indenter) is shown in Fig. 8. The indentation hardness of the equiaxed α and β (α') phases increased with increasing heat treatment temperature. The increase in the indentation hardness of the equiaxed α phase was significant compared to that of the β (α') phase, and the hardness difference between the equiaxed α and β (α') phases increased with increasing heat treatment temperature in the α+β region.

4. Discussion

4.1 Microstructure

The TEM images of the acicular structure observed in the specimens heat-treated in the α+β region at 1073 and 1173 K are shown in Fig. 9. After heat treatment at 1073 K, a parallel dislocation arrangement was observed in the acicular structure. This structure was introduced during the formation of α' martensite[12,13]. Therefore, the acicular struc-

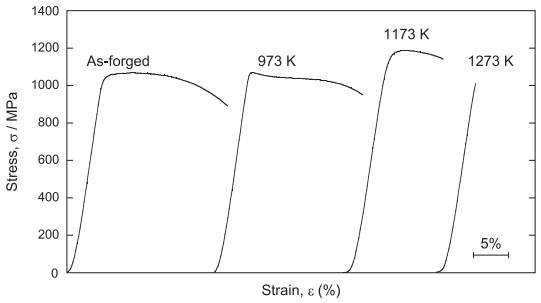

Fig. 5 Stress-strain curves of the as-forged and heat-treated alloy.

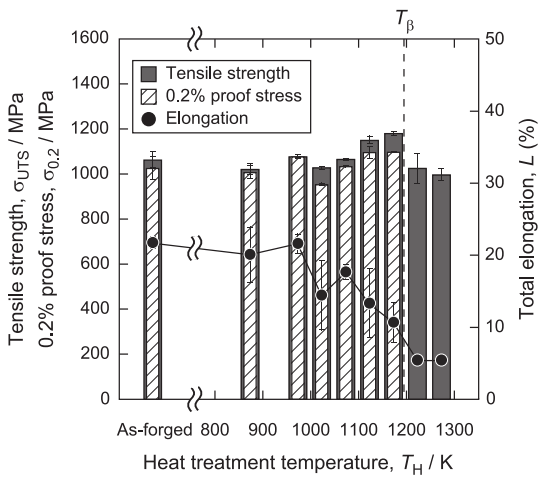

Fig. 6 Tensile strength, 0.2% proof stress, and total elongation of the as-forged and heat-treated alloy.

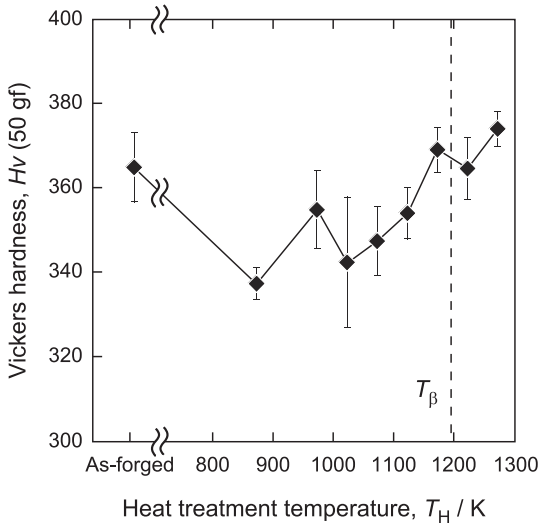

Fig. 7 Relationship between the heat treatment temperature and Vickers hardness of the as-forged and heat-treated alloy.

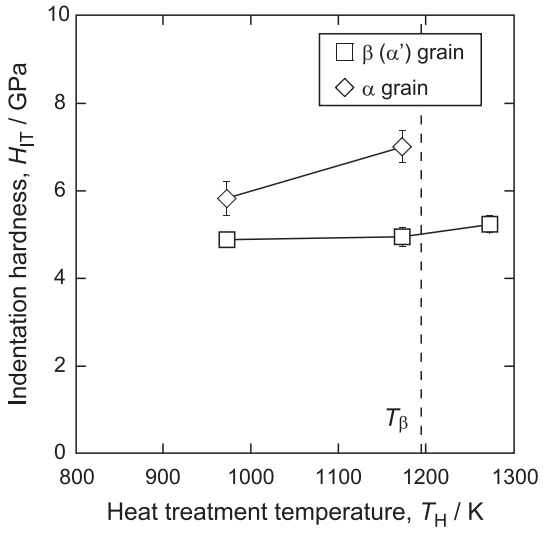

Fig. 8 Relationship between the heat treatment temperature and nano-indentation hardness of the equiaxed α and β (α') grains.

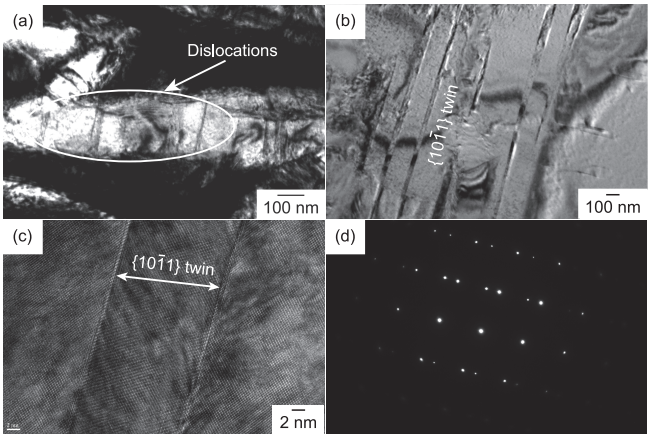

Fig. 9 Transmission electron microscopy (TEM) bright field images of the alloy heat-treated at (a) 1073 K and (b) 1173 K. (c) High resolution (HR) TEM image and (d) electron diffraction pattern of the alloy heat-treated at 1173 K.

ture which formed after heat treatment at 1073 K was confirmed to consist of α' martensite. The same dislocation arrangement was not observed in the acicular structure after heat treatment at 1173 K. However, as shown in the HRTEM image (Fig. 9(c)) and selected area diffraction pattern (Fig. 9(d)), {10$\bar{1}$1} twins (which also appear during α' martensite formation[14–16]) were observed.

The XRD patterns (Fig. 3) revealed that peak separation occurred after heat treatments at 1073 and 1123 K. Matsumoto *et al.*[14] reported that peak separation of the hcp phase was observed in a Ti-6Al-4V alloy when the equiaxed α phase and α' martensite coexist in the microstructure. Since α' martensite has the same chemical composition as the β phase prior to quenching, the V content in the α' martensite is higher than that in the equiaxed α phase. The V content difference between the equiaxed α and β phases was also found to increase with decreasing heat treatment temperature, as shown in Fig. 4(b). It has been reported that the lattice constant of α' martensite decreases with increasing V content[17,18]. As the V content of the α' martensite formed in the specimens heat-treated at 1073 and 1123 K was higher than that of the equiaxed α phase, it is thought that the α' martensite peaks shifted to a higher 2θ angle and peak separation occurred. However, peak separation was not observed after heat treatment at 1173 K. In the alloy heat-treated at 1173 K, the difference in the V content between the equiaxed α and β phase was smaller than that measured after heat treatment at 1073 and 1123 K. While the difference in the V content between the equiaxed α and β phases after heat treatment at 1023 K was larger than that after heat treatment at 1073 and 1123 K, peak separation of the hcp phase was not observed; this is because α' martensite did not form during quenching from 1023 K, as discussed in the next paragraph.

It is known that α'' martensite forms during quenching when the V content in the β phase is over 9.4 mass%, whereas α' martensite forms below this value[19]. In this study, the lowest heat treatment temperature at which α' martensite formed during quenching was 1073 K; the V content in the β phase at this temperature was 7.41 mass%. As the V content in the β phase at 1023 K was 8.92 mass%, it was expected that α' martensite would have formed during quenching; however, this was not observed. It is known that the martensitic transformation start temperature (Ms) for α' martensite is lowered by an increasing V content in the β phase, and falling below room temperature when the V content exceeds 14.9 mass%[20]. In addition, Kim *et al.*[21] reported that the addition of O lowered the Ms value in a Ti-Nb alloy. Therefore, it is suggested that the Ms of the Ti-4V-0.6O alloy heat-treated at 1023 K fell to below room temperature due to the higher V content and an almost identical O content compared to those at 1073 K, thus preventing α' martensite formation. It has been reported that α'' martensite forms during quenching from 1073 to 1143 K in a Ti-6Al-4V alloy with the same V content and Al-equivalent as that used in these experiments[5,22–24]. Ohyama and Nishimura[25] reported that Al addition lowered the Ms of a Ti-V alloy, but not sufficiently to prevent the formation of α'' martensite. Therefore, it is suggested that the addition of O produces a greater reduction in the Ms than Al at the same Al-equivalent in a Ti-V alloy.

4.2 Mechanical properties

As shown in Fig. 6, the tensile strength of the alloy heat-treated from 1073 to 1173 K was higher than that of the as-forged alloy. This corresponds to the temperature range in which α' martensite forms during quenching. It is known that α' martensite increases the tensile strength of α+β type Ti alloys[26–28]. Therefore, the increase in the tensile strength can be attributed to the formation of α' martensite. After heat treatments at 1223 and 1273 K, the tensile strength decreased despite the formation of α' martensite. This phenomenon was also observed in the Ti-6Al-4V alloy after solution treatment. Morita *et al.*[27] reported that quenching from the β single phase region led to a decrease in the tensile strength and an increase in the hardness compared to that of the alloy quenched from the α+β region (1173 K). As shown in the stress-strain curves of the heat-treated alloys (Fig. 5), brittle behavior was observed in the alloys heat-treated in the β single phase region. The fracture surfaces of the specimens heat-treated at 1223 and 1273 K are shown in Fig. 10. The fracture surfaces revealed that brittle fracture occurred, which is in good agreement with the stress-strain curves obtained from the specimens. Further, the prior β grain size of the alloy heat-treated at 1273 K was 1 to 3 mm, which corresponded to the size of flat area observed in the fracture surface. This suggests that the fracture occurred at the boundaries of the coarse prior β grains. Therefore, it is thought that these β grains caused the brittle fracture and observed decrease in tensile strength[27].

The total elongation of the alloy decreased with increasing heat treatment temperature. The indentation hardness of equiaxed α and β (α') grains (Fig. 8) showed that the change in the indentation hardness of the β (α') grains with heat treatment temperature was smaller than that of the equiaxed α grains. As shown in Fig. 4(a), the O content in equiaxed α phase increased with increasing heat treatment temperature. It is well-known that the presence of O in Ti increases the hardness by solid-solution strengthening[7,8], and the degree of hardening follows a parabolic dependence on the O con-

tent[29,30]. This is in good agreement with the experimental results shown in Fig. 4(a). As mentioned above, the hardness difference between the equiaxed α and β (α') grains was greater in the alloy heat-treated at 1173 K (10.6% total elongation) than at 973 K (22% total elongation). Kang *et al.*[31] reported that the elongation of a Ti-4Cr alloy heat-treated in the α+β region was improved by decreasing the hardness difference between the α and β phases. Fukai *et al.*[32] also reported that decreasing the hardness difference between the equiaxed α and β phases led to an improvement in the elongation of an SP-700 (Ti-4.5Al-3V-2Fe-2Mo) alloy. Therefore, reduced total elongation in this alloy was likely a result of an increase in the hardness difference between the equiaxed α and β (α') phases, which is attributed to the increased O content of the equiaxed α phase.

The effect of the addition of a β stabilizer on the O content of α and β phases at 1173 K was calculated using the Thermo-Calc software, based on the CALPHAD method (Thermo-Calc Software AB, Stockholm, Sweden) in conjunction with the TTTI3 thermodynamic database. The O distribution coefficient (k_O), as calculated from the O content of each phase using a Ti-O pseudo-binary phase diagram with an addition of 1 at.% β stabilizer, is shown in Fig. 11. The value of k_O between the α and β phases, is defined by eq. (2):

$$k_O = \frac{C_{O,\alpha}}{C_{O,\beta}} \tag{2}$$

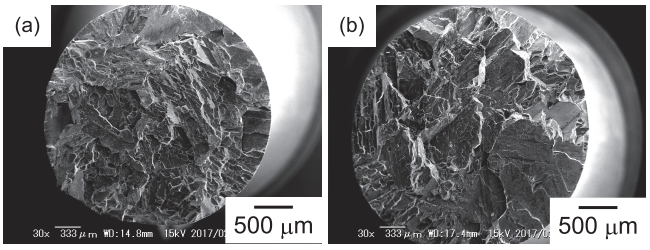

Fig. 10 Fracture surfaces of the alloy heat-treated at (a) 1223 K and (b) 1273 K.

where $C_{O,\alpha}$ and $C_{O,\beta}$ represent the O content in the α and β phases, respectively. As shown in Fig. 11, the addition of β stabilizer increased the value of k_O and enhanced the O distribution in the α phase. V and Nb are expected to possess lower k_O values compared with other β stabilizers such as Mo, Fe, and Cr. This indicates that the hardness difference between α and β phases could be suppressed in relation to V and Nb, which have a high O affinity. Therefore, V and Nb are effective β stabilizers when used in Ti-O alloys.

A comparison of the tensile strength and total elongation characteristics of the present Ti-4V-0.6O alloy and a Ti-6Al-4V alloy[33] is shown in Fig. 12, plotted as a function of the heat treatment temperature based on the T_β. The Ti-4V-0.6O alloy exhibits a tensile strength of over 1000 MPa after heat treatment in the α+β field, and a total elongation of 22% after heat treatment at 973 K, values which are comparable to those of the Ti-6Al-4V alloy. Further investigations into, for example, the effects of aging treatment on the mechanical properties, cold workability, and hot workability (including superplasticity) are required. However, this study indicates that the low-cost α+β type Ti-4V-0.6O has excellent strength and ductility characteristics, and demonstrates that low grade Ti sponge and scrap can be utilized as raw materials in its fabrication.

5. Conclusion

The microstructure and tensile properties of a newly designed Ti-4V-0.6O alloy were investigated with a focus on heat treatability. The following results were obtained.

(1) The β transus was determined from the approach curve to be 1195 K.
(2) α' martensite was detected in the transformed structure of the alloy heat-treated from 1073 to 1273 K.
(3) The V content in the β phase increased with increasing volume fraction of the equiaxed α phase, and the O content in the equiaxed α phase increased with decreasing equiaxed α phase volume fraction.
(4) Higher tensile strength and lower total elongation values were measured in the specimens heat-treated from 1073

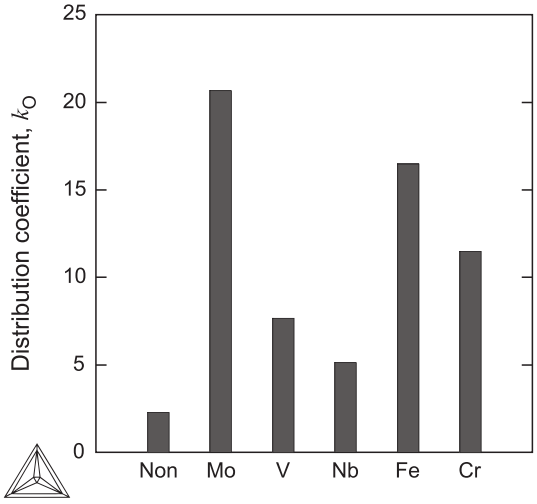

Fig. 11 Effect of elemental addition of 1 at.% β stabilizer on the O distribution coefficient at 1173 K in Ti, calculated using Thermo-Calc.

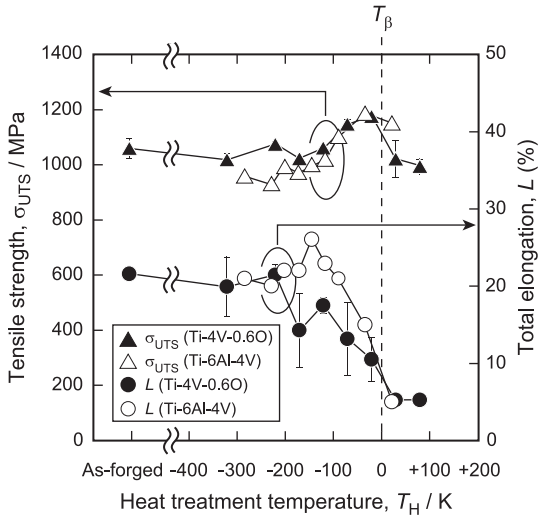

Fig. 12 Comparison of the tensile strength and total elongation of the Ti-4V-0.6O and Ti-6Al-4V alloys[33].

to 1173 K, as compared to the as-forged alloy. This was caused by the formation of α' martensite and an increase in the hardness difference between the equiaxed α and β (α' martensite) grains.

(5) The tensile strength and total elongation of the alloy were comparable to those of the Ti-6Al-4V alloy, and it is suggested that the Ti-4V-0.6O alloy can be used as a low-cost α+β type Ti alloy having excellent strength and ductility.

Acknowledgements

The authors would like to thank Dr. K. Kobayashi of Tohoku University for the TEM analyses. This study was partially supported by the Grant in Aid for Science Research from the Ministry of Education, Culture, Sports, Science and Technology (MEXT), Japan (Nos. 25249094 and 26709049), Iketani Science and Technology Foundation, and The Light Metal Educational Foundation, Inc.

REFERENCES

1) H. Kotaki: *On the technology of machining, plasticity processing, welding, processing of titanium*, (Nikkan Kogyo Shimbun Ltd., 2012) pp. 2–9, p. 21.
2) C. Ouchi: Bull. Jpn. Inst. Mat. **25** (1986) 672–679.
3) M. Niinomi: J. Jpn. Inst. Met. Mater. **75** (2011) 21–28.
4) T. Narushima: Titanium Japan **61** (2013) 126–131.
5) R. Boyer, E.W. Collings and G. Welsch: *Materials properties handbook: Titanium alloys*, (ASM, 1994) p. 10 and 490.
6) K. Takahashi and E. Sato: Tetsu-to-Hagané **98** (2012) 491–496.
7) Z. Liu and G. Welsch: Metall. Trans., A, Phys. Metall. Mater. Sci. **19** (1988) 527–542.
8) T. Hirano, T. Murakami, M. Taira, T. Narushima and C. Ouchi: ISIJ Int. **47** (2007) 745–752.
9) H. Fujii, K. Fujisawa, M. Ishii and Y. Yamashita: Nippon Steel Technical Report **375** (2001) 94–98.
10) H. Fujii: Titanium Japan **51** (2002) 33–37.
11) K. Ueda, T. Kobayashi and T. Narushima: J. Jpn. Inst. Met. Mater. **80** (2015) 60–65.
12) T. Ahmed and H.J. Rack: Mater. Sci. Eng. A **243** (1998) 206–211.
13) E.S.K. Menon and R. Krishnan: J. Mater. Sci. **18** (1983) 365–374.
14) H. Matsumoto, H. Yoneda, K. Sato, S. Kurosu, E. Maire, D. Fabregue, T.J. Konno and A. Chiba: Mater. Sci. Eng. A **528** (2011) 1512–1520.
15) J.C. Williams, R. Taggart and D.H. Polonis: Metall. Trans. **1** (1970) 2265–2270.
16) H.M. Flower, S.D. Henry and D.R.F. West: J. Mater. Sci. **9** (1974) 57–64.
17) W.B Pearson and G.H. Vineyard: *A handbook of lattice spacings and structures of metals and alloys*, (Pergamon Press, 1958) 872–877.
18) F.R. Brotzen, E.L. Harmon and A.R. Troiano: Trans. ASM **48** (1955) 774–782.
19) E.W. Collings: *The physical metallurgy of titanium alloys*, (ASM, 1984) p. 91.
20) P. Pietrokowsky and P. Duwez: Trans. Metall. AIME **194** (1952) 627–630.
21) J.I. Kim, H.Y. Kim, H. Hosoda and S. Miyazaki: Mater. Trans. **46** (2005) 852–857.
22) A.L. Kahveci and G.E. Welsch: Scr. Metall. **25** (1991) 1957–1962.
23) J.C. Williams and M.J. Blackburn: Trans. ASM **60** (1967) 373–383.
24) T. Morita and K. Murakami: Mater. Trans. **53** (2012) 173–178.
25) H. Ohyama and T. Nishimura: ISIJ Int. **35** (1995) 927–936.
26) P.J. Fopiano, M.B. Bever and B.L. Averbach: Trans. ASM **62** (1969) 324–332.
27) T. Morita, W. Niwayama, K. Kawasaki and Y. Misaka: Trans. JSME A **64** (1998) 2115–2120.
28) A. Ajiz, G. Gunawarman and J. Affi: IJASEIT **5** (2015) 329–334.
29) G. Conrad: Prog. Mater. Sci. **26** (1981) 123–403.
30) H.R. Ogden and R.I. Jaffee: TML Report No. 20, 1955.
31) D.S. Kang, N. Koga, M. Sakata, N. Nakada, T. Tsuchiyama and S. Takaki: Mater. Sci. Eng. A **606** (2014) 101–107.
32) H. Fukai, K. Minakawa and C. Ouchi: ISIJ Int. **44** (2004) 1911–1917.
33) R.G. Sherman and H.D. Kessler: Trans. ASM **48** (1956) 657–676.